RSC Advances



PAPER

View Article Online

View Journal | View Issue

Cite this: RSC Adv., 2014, 4, 14550

The one pot synthesis of heterobimetallic complexes from a homoditopic pyrimidine—hydrazone ligand†

Daniel J. Hutchinson, Lyall R. Hanton* and Stephen C. Moratti

The symmetrical, homoditopic, pyrimidine-hydrazone (pym-hyz) ligand L1 was used to synthesise three new heterobimetallic complexes, CuPbL1(ClO₄)₄, CuAgL1(SO₃CF₃)₃, and CuZnL1(SO₃CF₃)₄. Each of the complexes was produced in a one-pot reaction in CH₃CN, and was isolated in high yield and purity simply by precipitation through the addition of diethyl ether. Analysis was carried out by IR, UV-Vis and ESMS spectroscopy, as well as microanalysis. Crystals were also grown for the purposes of X-ray diffraction studies, which yielded the structures [CuPbL1(ClO₄)(CH₃CN)₂(H₂O)](ClO₄)₃ (1), [CuAgL1(SO₃CF₃)(CH₃CN)₂](SO₃CF₃)₂·CH₃CN (2), and CuZnL1(SO₃CF₃)₂(CH₃CN)(H₂O)](SO₃CF₃)₂·CH₃CN (3), all of which were linear complexes containing a Cu(III) ion in one of the pym-hyz-py coordination sites, and either a Pb(II), Aq(I), or Zn(II) ion in the other.

Received 18th December 2013 Accepted 4th March 2014

DOI: 10.1039/c3ra47735e

www.rsc.org/advances

Introduction

The cooperation of two different metal centres imbues heterobimetallic complexes with distinctly different physical and chemical properties from their mono- and homobimetallic analogues. As a result, synthetic heterobimetallics displaying novel properties have been extensively studied and exploited in the fields of catalysis, mixed spin magnetic systems, and molecular sensing and imaging. Additionally, they act as model compounds for studying the mechanisms and cooperative effects seen in important metalloenyzmes which utilise mixed metal ion active sites.

Supramolecular self-assembly can be employed to efficiently synthesise heterobimetallic complexes through the use of ditopic ligands with disparate metal binding sites which are selective towards different metal ions.⁶ The desired heterobimetallic complex can then be achieved by reacting the heteroditopic ligand with the metal ions in a sequential fashion. However, even with carefully designed heteroditopic ligands, these reactions often result in the formation of multiple complexes, necessitating yield limiting purification steps.⁷ Evidently, the synthesis of heterobimetallic complexes is not

trivial and is aided by an adept understanding of molecular recognition.

We have previously reported that the addition of Cu(u) ions

We have previously reported that the addition of $Cu(\pi)$ ions to a homoditopic pyrimidine-hydrazone (pym-hyz) ligand (L1) in a 1:1 metal to ligand ratio resulted in discrete Cu(L1H)- $(ClO_4)_3$ and $CuL1(SO_3CF_3)_2$ complexes in which one of the coordination sites was occupied by a $Cu(\pi)$ ion while the other one remained vacant (Fig. 1).8 Usually, ditopic pym-hyz ligands self-assemble into $[2 \times 2]$ grids when reacted with $Cu(\pi)$ ions in a 1:1 metal to ligand9 ratio as the terpyridine like pym-hyz-py coordination pockets are well suited to binding octahedral metal ions in a coplanar *mer* fashion. However, the addition of hydroxymethyl arms to the terminal py rings of L1 results in tetradentate coordination to the $Cu(\pi)$ ion, which prevents the perpendicular arrangement of ligand molecules required to form a grid complex.10

At the time of publication we envisioned that these monocopper L1 complexes could be useful precursors in the formation of heterobimetallic complexes. The facile synthesis of L1 and the high purity and yield at which the monocopper complexes are synthesised makes them readily accessible. Herein we report that reacting the $\text{Cu}(\text{L1H})(\text{ClO}_4)_3$ and $\text{CuL1}(\text{SO}_3\text{CF}_3)_2$ complexes with either Pb(II), Ag(I) or Zn(II) ions resulted in the formation of heterobimetallic $\text{CuM}^{n+}\text{L1A}_{(2+n)}$ complexes (where $\text{A} = \text{ClO}_4^-$ or SO_3CF_3^- ; Fig. 2). Each of the complexes was formed in a one pot reaction in which L1 was first mixed with a solution of Cu(II) ions, before a solution of the other metal ion was added. The heterobimetallic complexes were isolated in high yield without the need for extensive purification steps. They were characterised by microanalysis,

Department of Chemistry, University of Otago, PO Box 56, Dunedin, New Zealand. E-mail: lhanton@chemistry.otago.ac.nz

 $[\]dagger$ Electronic supplementary information (ESI) available: Crystallographic data for complexes 1–3 including a discussion of how disorder was handled, pictorial views with thermal ellipsoids at the 50% probability level and selected bond lengths and angles in tabulated form. CCDC 976905–976907. For ESI and crystallographic data in CIF or other electronic format see DOI: 10.1039/c3ra47735e

Paper **RSC Advances**

$$\begin{array}{c} \text{Cu}(\text{SO}_3\text{CF}_3)_2 \\ \text{CH}_3\text{CN} \end{array} \begin{array}{c} \text{N} \\ \text{N} \\ \text{N} \\ \text{N} \end{array} \begin{array}{c} \text{Cu}(\text{ClO}_4)_2 \\ \text{CH}_3\text{CN} \end{array}$$

Fig. 1 Solid state structures of the (right) $Cu(L1H)(ClO_4)_3$ and (left) $CuL1(SO_3CF_3)_2$ complexes synthesised by reacting L1 with either $Cu(ClO_4)_2$ or Cu(SO₃CF₃)₂ in a 1:1 metal to ligand ratio.8

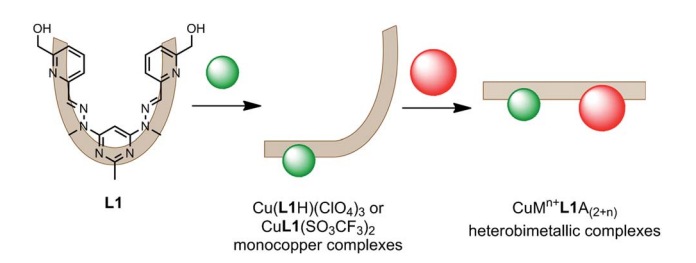


Fig. 2 The two step, one pot synthetic strategy employed to form the heterobimetallic $CuM^{n+}L1A_{(2+n)}$ complexes (where $M^{n+} = Pb(II)$, Ag(I) or Zn(II), and $A = ClO_4^-$ or $SO_3CF_3^-$).

mass spectrometry, IR and UV-Vis spectroscopy, and X-ray crystallography.

Results

Synthesis and analysis of complexes

The $CuM^{n+}L1A_{(2+n)}$ heterobimetallic complexes were all produced in high yields and purity by first synthesising the monocopper Cu(L1H)(ClO₄)₃ or CuL1(SO₃CF₃)₂ complexes, then filling the vacant coordination site with either a Pb(II), Ag(I) or Zn(II) ion (Fig. 2). As previously described, adding a CH₃CN solution of either Cu(ClO₄)₂·6H₂O or Cu(SO₃CF₃)₂·4H₂O to L1 in a 1:1 metal to ligand ratio resulted in dark green solutions of the monocopper complexes.8 Solutions of $Pb(ClO_4)_2 \cdot 3H_2O$, $AgSO_3CF_3$, or $Zn(SO_3CF_3)_2$ in CH_3CN in a 1 : 1 metal to ligand ratio were then added, and the heterobimetallic complexes were isolated as green precipitates simply by adding diethyl ether to the resulting solutions.

The microanalytical results from the $CuM^{n+}L1A_{(2+n)}$ precipitates were consistent with the formulae CuPbL1(ClO₄)₄, CuAgL1(SO₃CF₃)₃·CH₃CN and CuZnL1(SO₃CF₃)₄, while their ESMS spectra showed peaks due to either the [PbL1-H]⁺, [CuAgL1(SO₃CF₃)-H]⁺, or [CuL1-H]⁺ molecular ions, respectively. The IR spectra of the CuPbL1(ClO₄)₄, CuAgL1(SO₃CF₃)₃ and CuZnL1(SO₃CF₃)₄ complexes showed an O-H stretching mode at either 3449, 3436 or 3324 cm⁻¹, respectively, which were all typical frequencies of the $Cu(\pi)$, $Pb(\pi)$, $Ag(\pi)$ and $Zn(\pi)$ complexes of L1.8,11,12 The CuPbL1(ClO₄)₄ and CuAgL1(SO₃CF₃)₃ complexes each showed two C=N stretching modes, one of which was at 1565 cm⁻¹, while the other was at either 1541 or 1539 cm⁻¹. The CuZnL1(SO₃CF₃)₄ complex showed only the one C=N stretching mode at 1564 cm⁻¹, however it did have a distinct shoulder at 1554 cm⁻¹.

Samples of the complexes were dissolved in CH3CN and analysed by UV-Vis spectroscopy. Each of the complexes showed a single, broad, featureless d-d transition, in a similar fashion to the mono- and homobicopper L1 complexes.8 The d-d transitions of the CuPbL1(ClO₄)₄, CuAgL1(SO₃CF₃)₃ and CuZnL1- $(SO_3CF_3)_4$ complexes had λ_{max} values of either 697, 670, or 699 nm, and extinction coefficients of either 147, 144, or 135 L mol⁻¹ cm⁻¹, respectively. By comparison the transitions of the mono- and homobicopper complexes of L1 had λ_{max} values of 656 nm and 699 nm, respectively, with extinction coefficients of 170 and 250 L mol⁻¹ cm⁻¹, respectively.8

X-ray crystallography

Crystals of the $CuM^{n+}L1A_{(2+n)}$ complexes were also produced through the diffusion of diethyl ether vapour into the solutions, resulting in the solid state structures of [CuPbL1- $(ClO_4)(CH_3CN)_2(H_2O)[(ClO_4)_3 (1), [CuAgL1-(SO_3CF_3)(CH_3CN)_2] (SO_3CF_3)_2 \cdot CH_3CN$ (2), and $[CuZnL1-(SO_3CF_3)_2(CH_3CN) (H_2O)$](SO₃CF₃)₂·CH₃CN (3; Fig. 3–5). The overall structures of

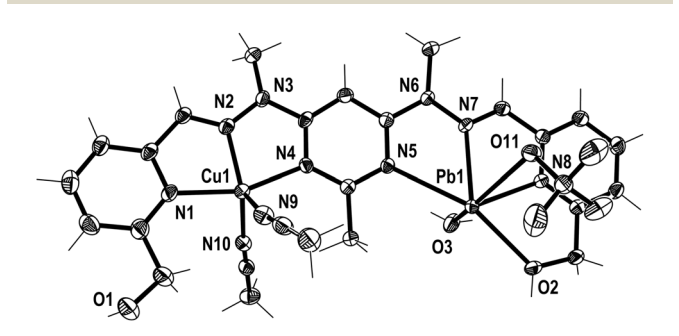


Fig. 3 View of the $[CuPbL1(ClO_4)(CH_3CN)_2(H_2O)]^{3+}$ cation of complex 1 (crystallographic numbering). Thermal ellipsoids are drawn at the 50% probability level.

N2 N3 N6 N7 N7 N8 N9 N9 N9 N9 N10 N10 O2

Fig. 4 View of the $[CuAgL1(SO_3CF_3)(CH_3CN)_2]^{2+}$ cation of complex 2 (crystallographic numbering). Thermal ellipsoids are drawn at the 50% probability level.

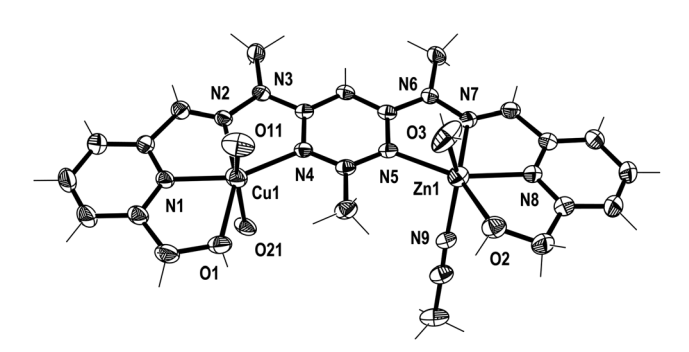


Fig. 5 View of the $[CuZnL1(SO_3CF_3)_2(CH_3CN)(H_2O)]^{2+}$ cation of complex 3 (crystallographic numbering). Thermal ellipsoids are drawn at the 50% probability level (the $SO_3CF_3^-$ anions coordinated to Cu1 have been simplified to O11 and O21 for clarity).

these complexes were similar to the previously reported Cu_2L1A_4 , Pb_2L1A_4 , Ag_2L1A_2 and Zn_2L1A_4 structures, as well as other pym-hyz ditopic complexes, in that they were linear with both pym-hyz-py bonds in the cisoid-cisoid conformation.^{8,11-13}

Additionally, in complexes 1 and 2, the halves of L1 which were bound to the Cu(II) ions were slightly curved in the mean plane of the central pym ring, while the halves bound to either Pb(II) or Ag(I) were straighter, as seen previously in the homobimetallic L1 complexes.8,11,12 As a result the lengths of complexes 1 and 2, 13.45 and 13.19 Å, respectively, were longer than the curved Cu₂L1A₄⁸ complexes but shorter than the straight Pb2L1A411 and Ag2L1A212 complexes. Both halves of complex 3 were slightly curved in the plane of the central pym ring, resulting in a length of 12.82 Å, which was slightly longer than the Cu₂L1A₄ complexes and similar in length to the curved Zn₂L1(SO₃CF₃)₄ complex. The intermetallic distances of complexes 1, 2 and 3 were 6.55, 6.36 and 6.11 Å, respectively, which were longer than the Cu-Cu distances previously reported for L1 homobimetallic complexes, but shorter than the Pb-Pb, Ag-Ag and Zn-Zn distances.8,11,12

The crystal structures of the monocopper complexes of L1 all contained a Cu(II) ion bound to the hydroxymethyl arm and N donors of L1 in a tetradentate fashion.⁸ However, when comparing complexes 1-3 it appeared that the tendency of the

hydroxymethyl arm to bind to the $Cu(\pi)$ ion was controlled by whether the other hydroxymethyl arm was bound to the other metal ion. In complex 1 the $Cu(\pi)$ ion was not bound to the hydroxymethyl arm, while the $Pb(\pi)$ ion was, as has been consistently observed in other $Pb(\pi)$ L1 complexes. Conversely, in complex 2 the hydroxymethyl arm was coordinated to the $Cu(\pi)$ ion, but not to the $Ag(\tau)$ ion, which commonly does not bind to the hydroxymethyl arms of L1. The asymmetric binding behaviour of the hydroxymethyl arms of L1 was previously observed in the Cu_2L1A_4 complexes in which only one of the $Cu(\pi)$ ions in each complex was bound to the hydroxymethyl arms. In contrast, complex 3 had the hydroxymethyl arms bound to both the $Cu(\pi)$ and $Zn(\pi)$ ions.

In addition to the hydroxymethyl arms, each of the metals in 1-3 was bound to the three N donors of the pym-hyz-py sites, CH₃CN solvent molecules, H₂O molecules and either ClO₄ or SO₃CF₃ anions. The Cu(II) ions in 1 and 2 adopted either a distorted trigonal bipyrimidal ($\tau_5 = 0.59$)¹⁴ or perfect square pyramidal ($\tau_5 = 0.01$)¹⁴ geometry, respectively. The Cu(II) ion in complex 3 had an octahedral geometry which was tetragonally distorted, with elongated bonds to the axially positioned SO₃CF₃⁻ anions, as is typical of Jahn-Teller distorted octahedral Cu(II) ions. 15 The geometries of the Pb(II) and Zn(II) ions in 1-3 were typical of other Pb(II), and Zn(II) complexes of L1. The Pb(II) ion in 1 adopted a six coordinate geometry, which resembled a distorted pentagonal bipyrimid due to the presence of a stereochemically active lone pair of electrons, 16 while the Zn(II) ion in 3 was present in a distorted octahedral geometry. The Ag(1) ion in 2 occupied a distorted square pyramidal environment $(\tau_5 = 0.25)$, which is a coordination geometry rarely displayed by Ag(I) ions.17

Both complexes **1** and **3** displayed H-bonding networks which arranged them into one dimensional chains (Fig. 6 and 7) while complex **2** was H-bonded into dimers (Fig. 8). The $[\text{CuPbL1}(\text{ClO}_4)(\text{CH}_3\text{CN})_2(\text{H}_2\text{O})]^{3+}$ cations of complex **1** were joined by H-bonds between one of the ClO_4^- counterions, and the hydroxymethyl arm, and the ClO_4^- and the H_2O molecule, both of which were bound to the $\text{Pb}(\pi)$ ion. Additionally, there

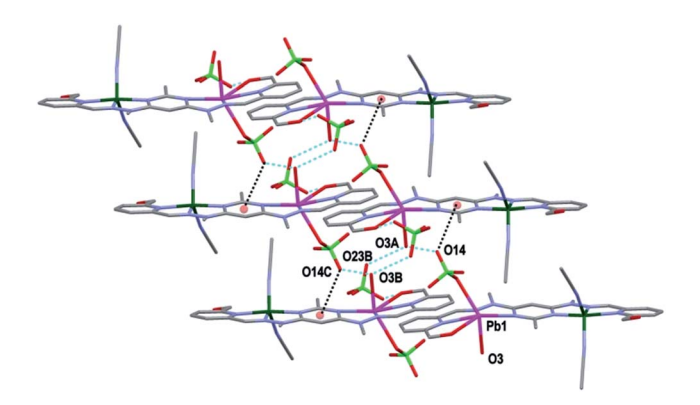


Fig. 6 View of the arrangement of complex 1 into a one dimensional chain in the [1 0 0] direction through H-bonding. The anion- π interaction between O14 and the central pym rings is also shown (hydrogens have been omitted for clarity; symmetry codes (A) -1 + x, y, z; (B) -x, 1 - y, -z).

Paper RSC Advances

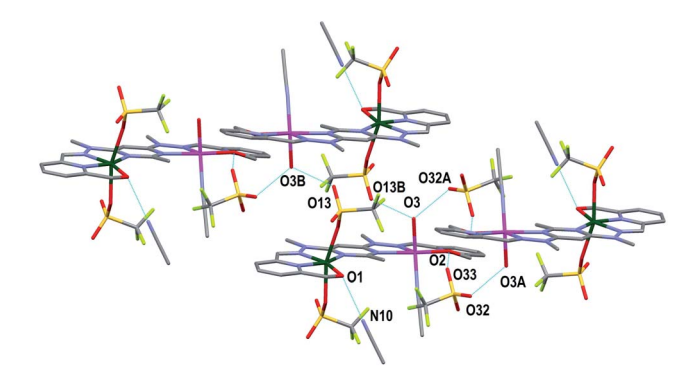


Fig. 7 View of the arrangement of complex 3 into a one dimensional chain in the [1 0 0] direction through H-bonding. The H-bonding interaction between O1 and a CH₃CN molecule is also shown (hydrogens have been omitted for clarity; symmetry codes A: -x, -y, 1-z; B: 1-x, -y, 1-z).

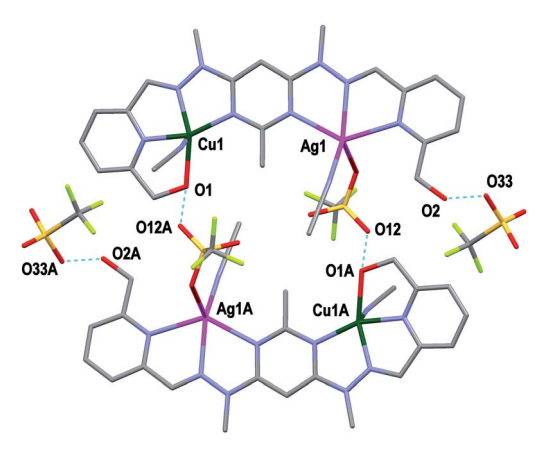


Fig. 8 View of two $[\text{CuAgL1}(\text{SO}_3\text{CF}_3)(\text{CH}_3\text{CN})_2]^{2+}$ cations of complex 2 joined as a dimer through H-bonding. Also shown is the H-bonding between O2 and the third SO_3CF_3^- anion (symmetry codes A: 2-x, 1-y, 1-z).

was an intermolecular anion– π interaction¹⁸ in complex 1 between the ClO₄⁻ anion bound to Pb1 and the central pym ring of **L1**. The distance from O14 to the centroid of the pym ring was 3.159(7) Å (Fig. 6). The H-bonding network of complex 3 involved bonds between the H₂O molecules coordinated to Zn(II), the SO₃CF₃⁻ anion bound to Cu(II) in a neighbouring [CuZnL1(SO₃CF₃)₂(CH₃CN)(H₂O)]²⁺ cation, and a free SO₃CF₃⁻ anion which was in turn H-bonded to one of the hydroxymethyl arms of another [CuZnL1(SO₃CF₃)₂(CH₃CN)(H₂O)]²⁺ cation. The other hydroxymethyl arms were H-bonded to a CH₃CN molecule. The [CuAgL1(SO₃CF₃)(CH₃CN)₂]²⁺ cations of complex 2 were paired into dimers by H-bonding between the hydroxymethyl arm coordinated to Cu(II) and the SO₃CF₃⁻ anion coordinated to Ag(I) (Fig. 8).

Experimental

General

All metal salts were purchased from commercial sources and were used as received without further purification with the exception of $\text{Cu}(\text{SO}_3\text{CF}_3)_2 \cdot 4\text{H}_2\text{O}$, which was produced by the treatment of $\text{Cu}(\text{CO}_3 \cdot \text{Cu}(\text{OH})_2 \cdot \text{H}_2\text{O}$ with aqueous triflic acid. Ligand L1 was synthesised according to its literature method.⁸ All solvents were used as received, and were of LR grade or better.

Microanalyses were carried out in the Campbell Microanalytical Laboratory, University of Otago. All measured microanalysis results had an uncertainty of ± 0.4 . Electrospray mass spectrometry (ESMS) was carried out on a Bruker microTOFQ instrument (Bruker Daltronics, Bremen, Germany) by employing direct infusion into an ESI source in positive mode. Infrared (IR) spectra were recorded on a Bruker Alpha-P ATR-IR spectrometer. UV-Vis spectra were recorded on an Agilent 8453 spectrophotometer against a CH₃CN background using quartz cells with a 1 cm path length.

CuPbL1(ClO₄)₄

Cu(ClO₄)₂·6H₂O (28.4 mg, 0.0768 mmol) was dissolved in CH₃CN (2.00 mL) and added to a suspension of L1 (32.0 mg, 0.0762 mmol) in CH₃CN (2.00 mL) stirring at 75 °C. This resulted in complete dissolution of the ligand material and the formation of a clear, green solution. Pb(ClO₄)₂·3H₂O (37.1 mg, 0.0807 mmol) in CH₃CN (2.00 mL) was then added to the stirring solution at 75 °C. The solution was cooled to rt and diethyl ether (20.0 mL) was added, resulting in the precipitation of a green solid. The solid was washed with diethyl ether and dried in vacuo (63.9 mg, 78%): Anal. found: C 23.42; H 2.76; N 10.41. Calc. for C₂₁H₂₄N₈O₁₈Cl₄CuPb: C 23.16; H 2.22; N 10.29. ESMS m/z found: 627.1653. Calc. for $C_{21}H_{23}N_8O_2Pb^+$: 627.1707. Selected IR ν cm⁻¹: 3449br (OH), 3067w (CH), 1600m, 1565m, 1541s (C=N), 1497m, 1431m, 1386w, 1289m, 1269m, 1158m, 1032s (ClO₄⁻). UV-Vis (CH₃CN) $\lambda_{\text{max}}(\varepsilon)/\text{nm}$ (L mol⁻¹ cm⁻¹): 697 (147). Green crystals suitable for X-ray determination were grown by the slow diffusion of diethyl ether into a CH3CN solution of Cu(ClO₄)₂·6H₂O, Pb(ClO₄)₂·3H₂O and L1 in a 1:1:1 ratio. These crystals gave the structure [CuPbL1- $(ClO_4)(CH_3CN)_2(H_2O)](ClO_4)_3$ (1).

$CuAgL1(SO_3CF_3)_3$

As described for CuPbL1(ClO₄)₄ but with Cu(SO₃CF₃)₂·4H₂O (32. 3 mg, 0.0745 mmol), L1 (29.5 mg, 0.0701 mmol), and AgSO₃CF₃ (20.5 mg, 0.0801 mmol); green solid (58.8 mg, 83%): Anal. found: C 29.12; H 2.69; N 11.50. Calc. for $C_{24}H_{24}N_8O_{11}F_9S_3CuAg \cdot CH_3CN$: C 28.91; H 2.52; N 11.67. ESMS m/z found: 737.9842, 482.1249. Calc. for $C_{21}H_{23}N_8O_2$ - $CuAg(SO_3CF_3)^+$: 737.9811. Calc. for $C_{21}H_{23}N_8O_2Cu^+$: 482.1240. Selected IR ν cm⁻¹: 3436br (OH), 3068w (CH), 1619m, 1599m, 1565m (C=N), 1539m (C=N), 1485m, 1456m, 1430m, 1384m, 1272s, 1235s (SO₃CF₃⁻), 1220s, 1152s, 1045m, 1023s. UV-Vis (CH₃CN) λ_{max} (ε)/nm (L mol⁻¹ cm⁻¹): 670 (144). Green crystals suitable for X-ray determination were grown by the slow diffusion of diethyl ether into a CH3CN solution of $Cu(SO_3CF_3)_2 \cdot 4H_2O$, AgSO₃CF₃, and L1 in a 1:1:1 ratio. These crystals gave the structure $[CuAgL1(SO_3CF_3)(CH_3CN)_2]$ - $(SO_3CF_3)_2 \cdot CH_3CN$ (2).

Table 1 Crystallographic data

	1	2	3
Formula	$\mathrm{C}_{25}\mathrm{H}_{32}\mathrm{Cl}_{4}\mathrm{CuN}_{10}\mathrm{O}_{19}\mathrm{Pb}$	$C_{30}H_{33}AgCuF_{9}N_{11}O_{11}S_{3}$	$C_{29}H_{32}CuF_{12}N_{10}O_{25}S_4Zn_{10}$
M	1189.16	1162.26	1245.80
Crystal system	Triclinic	Triclinic	Triclinic
Space group	$Par{1}$	$Par{1}$	$Par{1}$
a/Å	8.8553(8)	10.0293(2)	13.2894(2)
$b/ ext{Å}$	12.1810(11)	14.0756(2)	13.8254(3)
c/Å	18.5657(16)	16.8259(3)	15.4186(2)
α/°	88.849(4)	70.9120(6)	91.4555(15)
β/°	84.339(4)	87.5816(6)	111.9600(15)
γ/°	76.798(5)	72.0006(6)	115.552(2)
V/\mathring{A}^3	1940.2(3)	2130.25(7)	2310.61(9)
Z	2	2	2
T/K	90(2)	90(2)	100(2)
$\mu \; mm^{-1}$	5.248	1.215	4.028
Reflections collected	25 898	51 464	52 974
Unique reflections (R_{int})	7205 (0.0221)	7879 (0.0295)	9368 (0.0295)
R1 indices $[I > 2\sigma(I)]$	0.0361	0.0299	0.0601
wR2 (all data)	0.1069	0.0749	0.1659
Crystal size/mm	0.50 imes 0.12 imes 0.11	$0.51 \times 0.46 \times 0.35$	$0.15 \times 0.13 \times 0.06$
Max theta	25.50	25.50	66.49
Goodness of fit	1.095	1.057	1.077

CuZnL1(SO₃CF₃)₄

As described for CuPbL1(ClO₄)₄ but with Cu(SO₃CF₃)₂·4H₂O (32.8 mg, 0.0758 mmol), L1 (31.2 mg, 0.0743 mmol), and $Zn(SO_3CF_3)_2$ (27.3 mg, 0.0752 mmol); green solid (58.3 mg, 69%): Anal. found: C 26.32; H 2.49; N 9.84. Calc. for $C_{25}H_{24}N_8O_{14}F_{12}S_4CuZn$: C 26.21; H 2.11; N 9.78. ESMS m/zfound: 482.1114. Calc. for C₂₁H₂₃N₈O₂Cu⁺: 482.1240. Selected IR ν cm⁻¹: 3324br (OH), 3087w (CH), 1602m, 1564m (C=N), 1489w, 1433w, 1387w, 1365w, 1272s, 1220s (SO₃CF₃⁻), 1155s, 1056m, 1023s. UV-Vis (CH₃CN) λ_{max} (ε)/nm (L mol⁻¹ cm⁻¹): 699 (135). Green crystals suitable for X-ray determination were grown by the slow diffusion of diethyl ether into a CH3CN solution of $Cu(SO_3CF_3)_2 \cdot 4H_2O$, $Zn(SO_3CF_3)_2$, and L1 in a 1:1:1 These crystals gave the structure CuZnL1- $(SO_3CF_3)_2(CH_3CN)(H_2O)](SO_3CF_3)_2 \cdot CH_3CN$ (3).

X-ray crystallography information

Crystallographic data are summarised in Table 1, while selected bond lengths and angles for complexes 1–3 are available in the supporting information. X-ray diffraction data for complexes 1 and 2 were collected on a Bruker APEX II CCD diffractometer, with graphite monochromated Mo-K α ($\lambda=0.71073$ Å) radiation. Intensities for complexes 1 and 2 were corrected for Lorentz polarisation effects and a multiscan absorption correction was applied. The X-ray diffraction data for complex 3 were collected on an Agilent Supernova dual radiation source XRD with an Atlas detector and mirror monochromated Cu ($\lambda=1.5418$ Å) radiation. The data for complex 3 was processed using Agilent CrysAlisPro software (version 1.171.36), and an analytical absorption correction was applied.

The structures of complexes 1–3 were solved by direct methods (SHELXS²³ or SIR-97²⁴) and refined on F^2 using all data

by full-matrix least-squares procedures (SHELXL 97²⁵). All calculations were performed using the WinGX interface.²⁶ Detailed analyses of the extended structure were carried out using PLATON²⁷ and MERCURY²⁸ (Version 2.4).

Conclusions

The hetereobimetallic complexes CuPbL1(ClO₄)₄, CuAgL1-(SO₃CF₃)₃, and CuZnL1(SO₃CF₃)₄ were synthesised by reacting the homoditopic ligand, L1, with either Cu(ClO₄)₂·6H₂O or $Cu(SO_3CF_3)_2 \cdot 4H_2O$, followed by either $Pb(ClO_4)_2 \cdot 3H_2O$, AgSO₃CF₃, or Zn(SO₃CF₃)₂. The reactions were carried out in CH₃CN, in a one pot reaction, and the heterobimetallic complexes were isolated in high yield and purity simply by precipitating them out of solution through the addition of diethyl ether. Crystals of the complexes were also grown through vapour diffusion of diethyl ether. The X-ray diffraction studies of these showed the solid state structure of the complexes were all linear, with a Cu(II) ion in one coordination pocket and either a $Pb(\Pi)$, Ag(I) or $Zn(\Pi)$ ion in the other. The ability of L1 to produce these complexes in high yield and purity from one pot reactions, despite its symmetrical, homoditopic nature, makes it an interesting addition to the array of ligands currently employed to synthesise heterobimetallic complexes.

Acknowledgements

We thank the Department of Chemistry, University of Otago and the New Economic Research Fund of the Foundation for Research, Science and Technology (NERF Grant No UOO-X0808) for financial support. Notes and references

Paper

- 1 (a) B. G. Cooper, J. W. Napoline and C. M. Thomas, *Catal. Rev.: Sci. Eng.*, 2012, **54**, 1–40; (b) D. Astruc, E. Boisselier and C. Ornelas, *Chem. Rev.*, 2010, **110**, 1857–1959; (c) V. Ritleng and M. J. Chetcuti, *Chem. Rev.*, 2007, **107**, 797–858; (d) N. Wheatley and P. Kalck, *Chem. Rev.*, 1999, **99**, 3379–3420; (e) D. W. Stephan, *Coord. Chem. Rev.*, 1989, **95**, 41–107.
- (a) W. Guan, S. Yamabe and S. Sakaki, *Dalton Trans.*, 2013,
 42, 8717–8728; (b) S. Gu, D. Xu and W. Chen, *Dalton Trans.*, 2011, 40, 1576–1583; (c) A. Zanardi, J. A. Mata and E. Peris, *J. Am. Chem. Soc.*, 2009, 131, 14531–14537; (d) S. Maggini, *Coord. Chem. Rev.*, 2009, 253, 1793–1832; (e) A. Fihri, V. Artero, M. Razavet, C. Baffert, W. Leibl and M. Fontecave, *Angew. Chem., Int. Ed.*, 2008, 47, 564–567.
- 3 (a) S. Öz, J. Titiš, H. Nazir, O. Atakol, R. Boča, I. Svoboda and H. Fuess, *Polyhedron*, 2013, **59**, 1–7; (b) J. Černák, I. Kočanová and M. Orendá, *Comments Inorg. Chem.*, 2012, **33**, 2–54; (c) T. D. Pasatoiu, C. Tiseanu, A. M. Madalan, B. Jurca, C. Buhayon, J. P. Sutter and M. Andruh, *Inorg. Chem.*, 2011, **50**, 5879–5889.
- 4 (a) C.-F. Chow, M. H. W. Lam and W.-Y. Wong, *Anal. Chem.*,
 2013, 85, 8246–8253; (b) A. Boulay, S. Laine, N. Leygue,
 E. Benosit, S. Laurent, L. V. Elst, R. N. Muller, B. Mestre-Voegtle and C. Picard, *Tetrahedron Lett.*, 2013, 54, 5395–5398.
- 5 (a) L. M. K. Dassama, A. K. Boal, C. Krebs, A. C. Rosenzweig and J. M. Bollinger, J. Am. Chem. Soc., 2012, 134, 2520-2523;
 (b) P. A. Lindahl, Inorg. Biochem., 2012, 172-178; (c)
 V. R. I. Kaila, M. I. Verkhovsky and M. Wikström, Chem. Rev., 2010, 110, 7062-7081; (d) W. Jiang, D. Yun, L. Saleh, E. W. Barr, G. Xing, L. M. Hoffart, M. A. Maslak, C. Krebs and J. M. Bollinger, Science, 2007, 316, 1188-1191; (e)
 J. A. Tainer, E. D. Getzoff, J. S. Richardson and D. C. Richardson, Nature, 1983, 306, 284-287.
- 6 (a) S. K. Goforth, R. C. Walroth and L. McElwee-White, *Inorg. Chem.*, 2013, 52, 5692–5701; (b) M. R. Halvagar, B. Neisen and W. B. Tolman, *Inorg. Chem.*, 2013, 52, 793–799; (c) R. Maity, H. Koppetz, A. Hepp and F. E. Hahn, *Inorg. Chem.*, 2013, 135, 4966–4969; (d) N. Wang, J.-S. Lu, T. M. McCormick and S. Wang, *Dalton Trans.*, 2012, 41, 5553–5561; (e) Z.-L. You, Y. Lu, N. Zhang, B.-W. Ding, H. Sun, P. Hou and C. Wang, *Polyhedron*, 2011, 30, 2186–2194; (f) D. Huang and R. H. Holm, *J. Am. Chem. Soc.*, 2010, 132, 4693–4701; (g) D. L. M. Suess and J. C. Peters, *Chem. Commun.*, 2010, 46, 6554–6556.
- 7 (a) Y. Sano, A. C. Weitz, J. W. Ziller, M. P. Hendrich and A. S. Borovik, *Inorg. Chem.*, 2013, 52, 10229–10231; (b)
 C. Uyeda and J. C. Peters, *Chem. Sci.*, 2013, 4, 157–163.
- 8 D. J. Hutchinson, L. R. Hanton and S. C. Moratti, *Inorg. Chem.*, 2010, 49, 5923–5934.
- 9 (a) N. Parizel, J. Ramírez, C. Burg, S. Choua, M. Bernard, S. Gambarelli, V. Maurel, L. Brelot, J.-M. Lehn, P. Turek and A.-M. Stadler, *Chem. Commun.*, 2011, 47, 10951–10953;

- (b) A. R. Stefankiewicz, J. Harrowfield, A. Madalan, K. Rissanen, A. N. Sobolev and J.-M. Lehn, *Dalton Trans.*, 2011, 40, 12320–12332.
- 10 (a) L. N. Dawe, K. V. Shuvaev and L. K. Thompson, *Chem. Soc. Rev.*, 2009, 38, 2334–2359; (b) M. Ruben, J. Rojo, F. J. Romero-Salguero, L. H. Uppadine and J.-M. Lehn, *Angew. Chem., Int. Ed.*, 2004, 43, 3644–3662.
- 11 D. J. Hutchinson, L. R. Hanton and S. C. Moratti, *Inorg. Chem.*, 2011, **50**, 7637–7649.
- 12 D. J. Hutchinson, S. A. Cameron, L. R. Hanton and S. C. Moratti, *Inorg. Chem.*, 2012, **51**, 5070–5081.
- 13 A.-M. Stadler, N. Kyritsakas, R. Graff and J.-M. Lehn, *Chem. –Eur. J.*, 2006, **12**, 4503–4522.
- 14 A. W. Addison, T. N. Rao, J. Reedijk, J. van Rijn and G. C. Verschoor, *Dalton Trans.*, 1984, 1349–1356.
- 15 (a) B. Murphy and B. J. Hathaway, Coord. Chem. Rev., 2009,
 243, 237-262; (b) B. J. Hathaway, in Comprehensive Coordination Chemistry: The synthesis, reactions, properties & applications of coordination compounds, ed. G. Wilkinson,
 R. Gillard and J. A. McCleverty, Pergamon Press, Oxford,
 1987, vol. 5, ch. 53, pp. 594-600; (c) H. A. Jahn and
 E. Teller, Proc. R. Soc. A, 1937, 161, 220-223.
- 16 (a) J. Harrowfield, Helv. Chim. Acta, 2005, 88, 2430–2432; (b) L. Shimoni-Livny, J. P. Glusker and C. W. Bock, Inorg. Chem., 1998, 37, 1853–1867.
- 17 (a) D. J. Hutchinson, M. P. James, L. R. Hanton and S. C. Moratti, *Inorg. Chem.*, 2014, 53, 2122–2132; (b) K. Chainok, S. M. Neville, C. M. Forsyth, W. J. Gee, K. S. Murray and S. R. Batten, *CrystEngComm*, 2012, 14, 3717–3726; (c) A. G. Young and L. R. Hanton, *Coord. Chem. Rev.*, 2008, 252, 1346–1386.
- 18 (a) T. J. Mooibroek, C. A. Black, P. Gamez and J. Reedijk, Cryst. Growth Des., 2008, 8, 1082–1093; (b) C. A. Black, L. R. Hanton and M. D. Spicer, Inorg. Chem., 2007, 46, 3669–3679.
- 19 (a) Z. Otwinowski and W. Minor, in Processing of X-Ray Diffraction Data Collected in Oscillation Mode, Methods in Enzymology, Molecular Crystallography, Part A, ed. C. W. Carter and R. M. Sweet, Academic Press, New York, 1997, vol. 276, pp. 307–326; (b) SAINT V4, Area Dectector Control and Integration Software, Siemens Analytical X-ray Systems Inc., Madison, 1996.
- 20 G. M. Sheldrick, *SADABS*, *Program for Absorption Correction*, University of Göttingen, Göttingen, Germany, 1997.
- 21 Agilent Technologies, *Xcalibur/Supernova CCD system, CrysAlisPro Software System, version 1.171.36.XX*, 2012, Agilent Technologies UK Ltd, Oxford, UK.
- 22 R. C. Clark and J. S. Reid, *Acta Crystallogr., Sect. A: Found. Crystallogr.*, 1995, **51**, 887–897.
- 23 G. M. Sheldrick, Acta Crystallogr., Sect. A: Found. Crystallogr., 1990, 46, 467–473.
- 24 A. Altomare, M. C. Burla, M. Camalli, G. L. Cascarano, C. Giacovazzo, A. Guagliardi, A. G. G. Moliterni, G. Polidori and R. Spagna, J. Appl. Crystallogr., 1999, 32, 115–119.
- 25 G. M. Sheldrick, *SHELXL-97, Program for the Solution of Crystal Structures*, University of Göttingen, Göttingen, Germany, 1997.

RSC Advances

- 26 L. J. Farrugia, J. Appl. Crystallogr., 1999, 32, 837-838.
- 27 A. L. Spek, Acta Crystallogr., Sect. A: Found. Crystallogr., 1990, 46, 153-165.
- 28 (a) C. F. Macrae, P. R. Edgington, P. McCabe, E. Pidcock, G. P. Shields, R. Taylor, M. Towler and J. van de Streek,

J. Appl. Crystallogr., 2006, 39, 453-457; (b) I. J. Bruno, J. C. Cole, P. R. Edgington, M. K. Kessler, C. F. Macrae, P. McCabe, J. Pearson and R. Taylor, Acta Crystallogr., Sect. B: Struct. Sci., 2002, 58, 389-397.